AMERICAN INSTITUTE OF MINING AND METALLURGICAL ENGINEERS
Technical Publication No. 1089
(CLASS C, IRON AND STEEL DIVISION, NO. 231; CLASS E, INSTITUTE OF METALS DIVISION, NO. 289)

Reaction Kinetics in Processes of Nucleation and Growth

BY WILLIAM A. JOHNSON* AND ROBERT F. MEHL,† MEMBER A.I.M.E.

(New York Meeting, February, 1939)

IT is now recognized that several important types of reactions in metallic systems proceed by the formation of nuclei and the growth of these nuclei. The process of freezing is a simple example of this, as Tammann pointed out years ago.[1] Tammann held that the rate of freezing is determined by a rate of nucleation, expressed as the number of nuclei formed per unit volume of unfrozen liquid per second, and a rate of growth of these nuclei, expressed as the linear rate of radial growth in units of length per second. For isothermal freezing the conception is simple; for ordinary freezing, extending over a range of temperature, it is not as simple, for the values of the two constants must change with change in temperature. There is ample evidence that the postulated mechanism is correct even though a quantitative derivation of the rate of isothermal or of ordinary freezing in terms of the two constants has been lacking.

In recent years other reactions have been found to proceed in a similar fashion. It has been well established, particularly by Bain,[2–8] that the formation of pearlite from the eutectoid decomposition of the solid solution austenite proceeds in such a way, and Polanyi and Schmid, Tammann and Crone, Karnop and Sachs, and others[9–11] have shown that the process of recrystallization proceeds in a similar way.

Isothermal reaction rates have been determined for eutectoid decomposition by a number of investigators. Bain's[2–8] work on the formation of pearlite from austenite is especially valuable in this respect—the type of isothermal reaction curve obtained, as illustrated in Fig. 13, showed an initial slow rate, accelerating to an intermediate maximum rate which then decelerated to the completion of the reaction; similar curves have been obtained by Wever and his collaborators.[12] Other eutectoid decompositions show similar behavior: for example, the decomposition of the beta eutectoid in the copper-aluminum system, studied by Smith

Manuscript received at the office of the Institute Dec. 1, 1938.

* Molybdenum Corporation of America Graduate Fellow, Department of Metallurgy, Carnegie Institute of Technology, Pittsburgh, Pa.

† Director, Metals Research Laboratory, and Head, Department of Metallurgy, Carnegie Institute of Technology, Pittsburgh, Pa.

[1] References are at the end of the paper.

and Lindlief;[13] of the beta eutectoid in the aluminum-zinc system;[14] and of the "FeO," wüstite, phase in the iron-oxygen system (in this case the initial slow rate is absent or minor).[15] The proeutectoid rejection of ferrite in the decomposition of austenite has certain similarities,[16] though this reaction is more nearly comparable to simple precipitation from a solid solution. The rates of allotropic changes in tin[17] and in sulphur[18] have been studied, but the data are not of general use, for nucleation in these cases, occurring chiefly on the surface of the sample, is dependent on the shape of the sample used and on the nature of the liquid in which the samples are immersed; the isothermal reaction curves are not readily reproducible.

The analysis of isothermal reaction curves is more readily made when there are no concentration changes in the unreacted matrix during the reaction, for such concentration changes will certainly cause a variation in the rate of nucleation or the rate of growth during the reaction, greatly complicating the analysis; the process of freezing of a pure metal or of a congruently freezing alloy, the process of recrystallization of a metal or alloy following cold-work, and the process of eutectoid decomposition of a solid solution phase, however, all proceed without concentration changes in the unreacted matrix. For such reactions, which thus include processes of great industrial and metallurgical importance, an analysis of the isothermal reaction curve is important, both for the purpose of providing an explanation for the exact form of the curve and of providing assistance in determining the values of the basically important factors of the rate of nucleation and the rate of growth.

It has been conventional in the past to compare such isothermal reaction curves with chemical reaction curves of various orders. Thus Chaudron and Forester[15] stated that the isothermal reaction rate for the decomposition of "FeO" varies with the fourth power of the percentage of undecomposed "FeO"; Bain[2–8] compared the isothermal reaction curve for the formation of pearlite from austenite with the first order chemical reaction curve, but also pointed out discrepancies in the comparison; similar comparisons have been made by Fraenkel and Goez[14] for the decomposition of the beta phase in the aluminum-zinc system and by McBride, Herty and Mehl[16] for the proeutectoid rejection of ferrite from austenite. Such comparisons are of little use. The rate of many reactions may be expressed as dependent upon the momentary value of some quantity, but though in some reactions this has been of assistance in discovering the underlying mechanism of the reaction, in others, among which are those being considered here, it is purely an empirical and approximate representation of rate data. In first order reactions in a single homogeneous phase, in gases or liquids, the dependence of the rate upon the momentary concentration of the reactant is explicable on the basis that the rate is determined by the probability of

the formation of activated molecules through the energy redistribution following favorable collision, and in such cases the quantities in the first order reaction equation have real meaning in terms of concentration of reactant and resultant. There are no true concentration variables in any of the reactions cited above (in the formation of pearlite from austenite, for example, there is no concentration variation within any phase throughout the progress of the reaction) and there is no fundamental similarity to any reaction proceeding in a homogeneous phase. The reactions considered here are heterogeneous reactions which proceed by nucleation and by growth at an interface; for such reactions it is obvious that a quantitative expression for the rate of decomposition derived by the use of quantities of real physical significance—namely, the rate of nucleation and the rate of growth—will be far more useful.

Various attempts have been made to describe the isothermal reaction curve in terms of certain constants; Krainer[19] proposes to superimpose a reaction curve of the first order on the isothermal curve for the formation of pearlite and to characterize the experimental curve by the rate constant for the first order reaction and by the time intercept of the first order reaction curve, which he designates as the "nucleation time"; such attempts, while perhaps somewhat useful for comparison among similar data, are of no analytical use because the terms have no real meaning.

J. B. Austin and R. L. Rickett[20] recently demonstrated that the isothermal reaction curve for the formation of bainite from austenite in eutectoid steels (isothermal reaction temperatures between 570° and 200° C.) and less certainly for the formation of pearlite can be plotted as straight lines "if time is plotted logarithmically and the percentage transformed on either the 'autocatalytic' or the 'integrated-probability' scale." As the authors point out, the result is empirical and not in terms of a known mechanism of reaction; it is of assistance in appraising the accuracy of rate data and in comparing rate data for different temperatures. There is no apparent relation between this result and the mechanism by which the reactions are believed to proceed.

Several writers have pointed out that isothermal reaction curves for different temperatures of reaction and for different alloy steels can be brought into approximate coincidence by displacement on the logarithmic time scale;[21–23] the coincidence is only fair, however, and, at the moment, of uncertain significance; it adds nothing to the knowledge of the basic factors determining the rate of reaction.

The only attempts to derive the isothermal curve in terms of rates of nucleation and growth thus far recorded are that by Göler and Sachs,[24] that by Tammann,[22] and that by Fraenkel and Goez.[18] Göler and Sachs assumed a constant rate of nucleation in a unit volume of untransformed matrix and a constant rate of radial growth of these nuclei to spheroids (and to other geometric forms). The analysis, however, did not allow

for the impingement of growing spheroids and the resultant retardation in the reaction rate—accordingly, it gave a rate continuously increasing with time; it assumed general nucleation, that is, nuclei forming at random positions in the matrix, and thus did not provide for nucleation at grain boundaries as often observed in the formation of pearlite. Tammann used a simple arithmetical method, which bore the same limitations; Tammann's selection of isothermal reaction curves for comparison from the work of Bain was unfortunate, for these curves apply to the formation of lower bainite, which appears not to proceed by a process of nucleation and growth.[25] Fraenkel and Goez attempted to calculate the rate of transformation in terms of the rate of nucleation and the rate of growth, but assumed all nuclei to form at the first instant and did not provide for impingement, though the factors that determine the full form of the isothermal reaction curve were accurately described in a qualitative way.

An analysis of the isothermal reaction curve thus requires an expression in terms of the rate of nucleation and the rate of growth. When nucleation is exclusively or largely at the grain boundary, it requires an additional term for the matrix grain size. Such analyses are presented herewith, which: (1) reproduce the form of the observed isothermal reaction curve, (2) permit predictions to be made concerning the influence of of the several variables on the rate of reaction and on the shape of the reaction curve, and (3) offer methods by which the determination of rates of nucleation and growth may be greatly facilitated.

General Nucleation

The Analysis

The following analysis pertains to reactions in which nuclei form at random throughout the matrix, without regard for the matrix structure. Such an analysis should apply to the process of congruent freezing and to recrystallization in pure metals and in one-phase alloys. It will be assumed in this derivation: (1) that the reaction proceeds by nucleation and growth; (2) that the rate of nucleation, N_v, expressed in number of nuclei per unit of time per unit of volume, and the rate of radial growth G, expressed in units of length per unit of time, are both constant throughout the reaction; (3) that nucleation is random, without regard for matrix structure; and (4) that the reaction product forms true spheres except when during growth impingement on other growing spheres occurs. Departures from these simple assumptions will be discussed later. The small volumes of reaction product grown from single nuclei will hereinafter be termed "nodules."

An expression for the extent of reaction at any reaction time in terms of N_v and G is required, which provides for the impingement of growing

nodules of reaction product and the resultant inactive impingement interface. The derivation of the equation is given in Appendix A.* This derivation is obtained by the following scheme: The rate of growth of a sphere nucleated at some arbitrary time is calculated; the rate of growth of an actual nodule—a sphere that has suffered impingement and thus distortion from sphericity during growth—is a fraction of the rate of growth of the sphere; this fraction is simply the fraction of untransformed matrix; this determines the rate of growth of one nodule, which, multiplied by the number of nodules nucleated at the same time, gives the rate of growth of all nodules nucleated at this arbitrary time; sum-

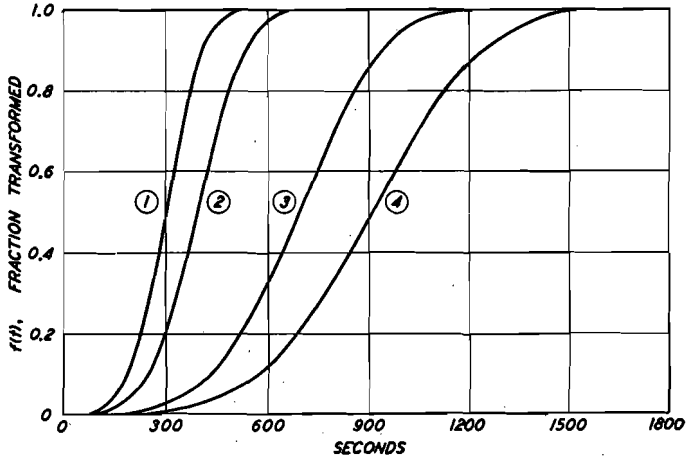

FIG. 1.—REACTION CURVES FOR GENERAL NUCLEATION FOR VARIOUS VALUES OF N_v AND G. ABSCISSA SCALE LINEAR.
Curve 1 is for $N_v = 3000$ per cm.^{3} per sec., $G = 3 \times 10^{-5}$ cm. per sec.
Curve 2 is for $N_v = 1000$ per cm.^{3} per sec., $G = 3 \times 10^{-5}$ cm. per sec.
Curve 3 is for $N_v = 3000$ per cm.^{3} per sec., $G = 1 \times 10^{-5}$ cm. per sec.
Curve 4 is for $N_v = 1000$ per cm.^{3} per sec., $G = 1 \times 10^{-5}$ cm. per sec.

ming such expressions for all times of nucleation gives the rate of transformation; integrating this expression gives an equation for the fraction transformed as a function of time, the expression required (equation 1):

$$f(t) = 1 - e^{-\frac{\pi}{3}N_v G^3 t^4} \qquad [1]$$

in which $f(t)$ is the fraction transformed and t is the time expressed in the same units as N_v and G.

Properties of the Plot

Equation 1 is plotted in Fig. 1 for a series of values of N_v and G, with $f(t)$ as ordinate and t as abscissa. It has become conventional to record

* The appendixes A, B, C, D, and E, in which are given the full details of the derivation of this and later equations may be obtained in the form of microfilm, from the American Documentation Institute, 2101 Constitution Avenue, Washington, D. C. The A.D.I. number is 1182 and the price $0.45 in microfilm and $2.70 in photoprint.

the time axis logarithmically on such diagrams in order that widely differing reaction curves may be plotted on a single diagram; Fig. 2 is such a plot.* These plots may be simplified by taking values of the quantity $\sqrt[4]{N_v G^3} \times t$ as abscissas, in which case one curve suffices to represent the family of curves in Figs. 1 and 2, as shown in Figs. 3 and 4.

The derivation obtained by Göler and Sachs[24] gives curves that are nearly identical with those in Figs. 1 to 4, up to about 5 per cent reaction (a difference of 0.1 to 0.2 per cent), but which differ increasingly at higher percentages of reaction.

It may be seen from Figs. 3 and 4 that the amount of transformation depends solely on the value of the term $\sqrt[4]{N_v G^3} \times t$ and not on individual

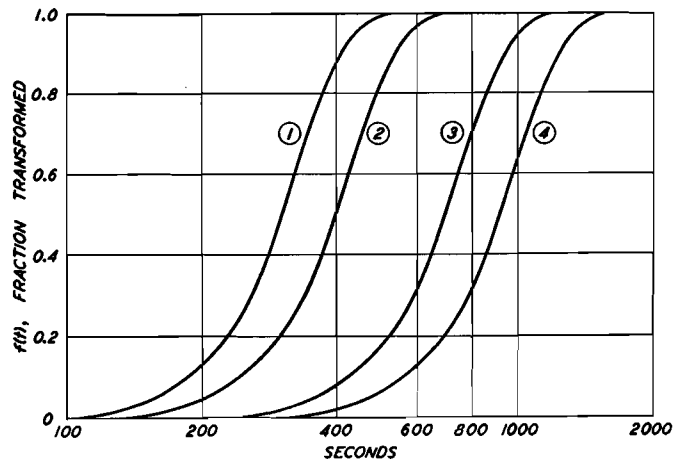

FIG. 2.—REACTION CURVES SHOWN IN FIG. 1, BUT WITH ABSCISSA SCALE LOGARITHMIC.

values of N_v, G, and t. Accordingly, identical reaction curves can be obtained for an infinite number of pairs of values of N_v and G for which the product $N_v G^3$ is the same. It follows that if two curves coincide at any point they coincide throughout.

The curves in Figs. 1 and 2 for various values of N_v and G all have the same shape: i.e., by contracting or extending the time axis linearly they can be brought into coincidence; this will be the criterion for shape. This is a characteristic of reactions that exhibit general nucleation, but not of

* Caution must be exercised in inspecting reaction curves plotted with time logarithmically, for the logarithmic plot distorts the curve, extending it at short time periods and condensing it at long. Plotted in this way, all reaction curves appear to start more slowly than they actually do—even a first order reaction curve, which begins with maximum velocity, appears when plotted this way to begin with a slow velocity and then to accelerate. It should also be noted that there is no zero on the logarithmic plot, and the displacement of a given curve to the right or the left depends solely on the logarithmic value chosen as the origin. These comments apply as well to the second section of this paper as to the first, and apply as well to experimental as to calculated curves.

reactions in which the locus of nucleation is dependent upon structure, as shown in the second section.

The relative effects of N_v and G upon the reaction curve may be seen in Figs. 1 and 2. A given change in the rate of growth exerts a much

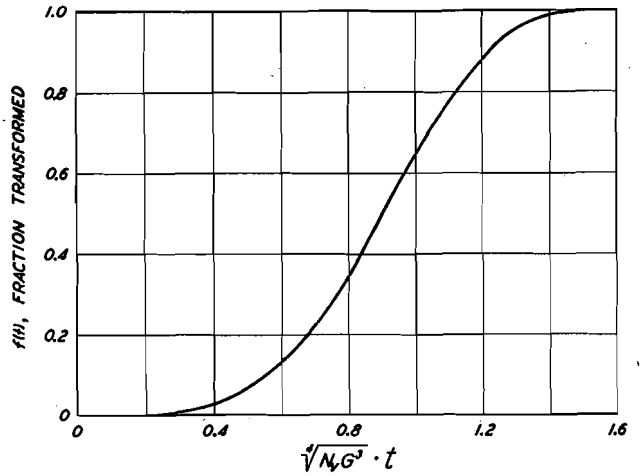

FIG. 3.—MASTER REACTION CURVE FOR GENERAL NUCLEATION, ABSCISSA SCALE LINEAR.

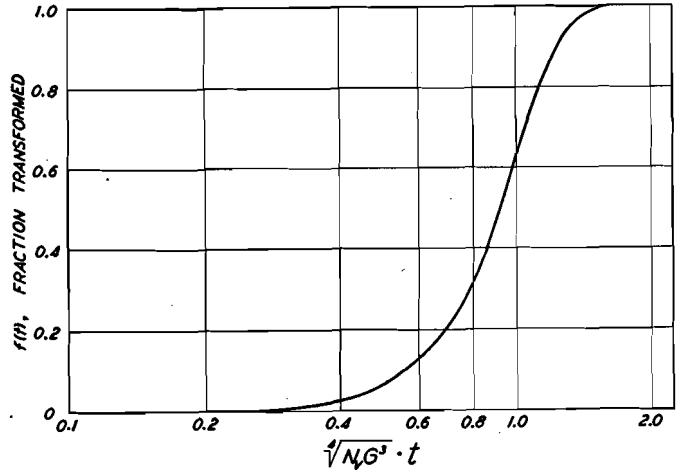

F G. 4.—MASTER REACTION CURVE FOR GENERAL NUCLEATION, ABSCISSA SCALE LOGARITHMIC.

greater influence on the reaction curve than a corresponding change in the rate of nucleation; this is evident from the fact that G occurs in the third power in the product $N_v G^3$ whereas N_v occurs in the first.

It is conceivable that the rate of growth of the nodules might vary with the crystal direction in the transforming phase. Such variation would lead to ellipsoids (or more complicated shapes) rather than spheres, but

the shape of the reaction curve would remain the same. The coefficient of t^4 in the exponential term of equation 1 would be changed, however, and the time of reaction would thus also be changed.

Effect of Variation in N_v and G during Reaction

It is known that in certain recrystallization processes (*vide infra*) N_v and G are not constant throughout the reaction; it is necessary, therefore, to study the effect of this variation upon the reaction curve. The derivation given in Appendix A can be modified to apply to any assumed varia-

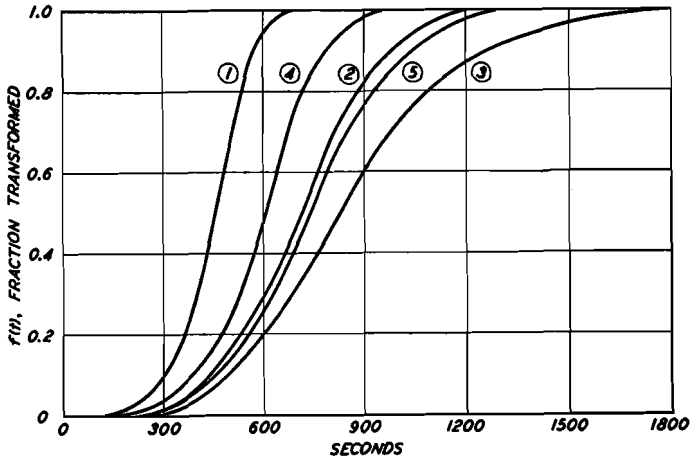

FIG. 5.—REACTION CURVES FOR GENERAL NUCLEATION SHOWING EFFECT OF VARIATIONS IN N_v AND G DURING REACTION.

Curve 1 is for G increasing linearly with time from 1×10^{-5} cm. per sec. at beginning of reaction to 3×10^{-5} at end (99.9 per cent), N_v constant, equal to 1000 per cm.^{3} per sec.

Curve 2 is for G, constant, equal to 1×10^{-5} cm. per sec., N_v, constant, equal to 1000 per cm.^{3} per sec.

Curve 3 is for G decreasing from 1×10^{-5} cm. per sec. at beginning of reaction to 0.33×10^{-5} cm. per sec. at end, N_v, constant, equal to 1000 per cm.^{3} per sec.

Curve 4 is for N_v increasing from 1000 per cm.^{3} per sec. at beginning of reaction to 10,000 at end, G constant, equal to 1×10^{-5} cm. per sec.

Curve 5 is for N_v decreasing from 1000 per cm.^{3} per sec. at beginning of reaction to zero at end G, constant, equal to 1×10^{-5} cm. per sec.

tion in N_v and G; one illustration of such a modification of the analysis is given in Appendix B. If it is assumed that N_v and G vary during reaction linearly with time in such a way that $N_v = N_{v0}\,(1 + \beta t)$ and $G = G_0\,(1 + \alpha t)$, in which α and β are constants, a suitable expression may be obtained (equation 2):

$$f(t) = 1 - \exp.\left\{-\pi N_0 G_0^3 \left[\frac{t^4}{3} + \frac{t^5}{15}(9\alpha + \beta) + \frac{t^6}{30}\alpha(11\alpha + 4\beta) + \frac{t^7}{210}\alpha^2(16\alpha + 19\beta) + \frac{t^8}{48}\alpha^3\beta\right]\right\} \quad [2]$$

Reaction curves for several values of α and β are plotted in Fig. 5. The effect of such variation in G on the shape of the reaction curve is shown in Fig. 6, in which three of the five curves of Fig. 5 are replotted, each on a different scale, in such a way that they coincide at 50 per cent reaction. Variation in G during the reaction gives different shapes to the curves. The curve for G increasing during the progress of the reaction, curve 1 lies below the reference curve (for which N_v and G are constant during the reaction) up to 50 per cent reaction and above, beyond 50 per cent; the curve for G decreasing during the reaction shows the opposite behavior. Variation in G during the reaction exerts a more marked influence on the reaction curve than variation in N_v; replotting

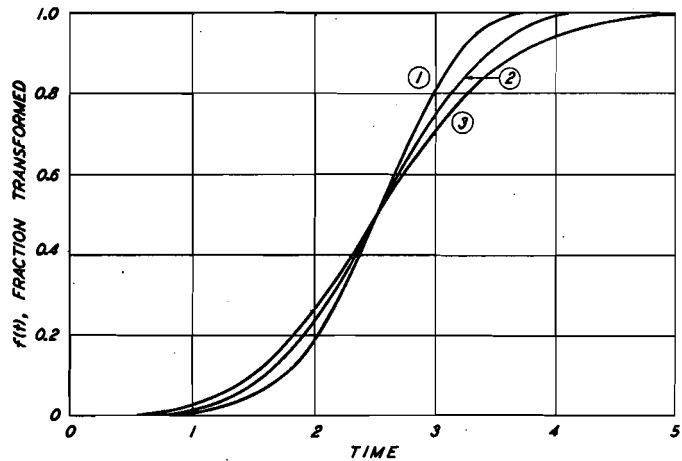

FIG. 6.—CURVES 1, 2 AND 3 OF FIG. 5 REPLOTTED ON ABSCISSA SCALES CHOSEN SO AS TO GIVE COINCIDENCE AT 50 PER CENT REACTION, SHOWING EFFECT OF VARIATIONS IN G DURING REACTION ON SHAPE OF REACTION CURVE.

curves 4 and 5 of Fig. 5 yields curves nearly indistinguishable from curve 2, and accordingly they are not replotted in Fig. 6.

Distribution of Nodule and Patch Sizes

It will be shown that the above expressions are useful in determining N_v and G. In applying them for this purpose, it will be convenient to consider the distribution of nodule sizes in space and of nodule areas, which we shall call "patches," on a plane of polish. The calculations that lead to the distribution functions given below are contained in full in Appendix C.

In the discussion to follow, the distribution function $P(x)$ of a set of objects whose characteristic measure (volume or radius) is x is defined in such a way that the number of objects with measure between x and $x + dx$ is $P(x)\,dx$. The distribution function, $\eta(\bar{\phi})$, of nodule volumes,

$\bar{\phi}$, for a completely reacted sample has been calculated by finding the number of nodules formed in a short time interval and the average volume of these nodules. This function is given by the parametric equations

$$\eta(\bar{\phi}) = \frac{(N_V/G)^{3/4} e^{-2\alpha^4}}{8\sqrt{3\pi}\int_\alpha^\infty e^{-v^4}[(v-\alpha) - 2\alpha^3(v-\alpha)^2]dv} \qquad [3]$$

$$\bar{\phi} = 4\sqrt[4]{27\pi}(G/N_V)^{3/4} e^{\alpha^4}\int_\alpha^\infty e^{-v^4}(v-\alpha)^2 dv$$

where α is the parameter and v is an integration variable. Equation 3 is plotted in Fig. 7; the method of plotting is described in detail in the discussion of Fig. 9.

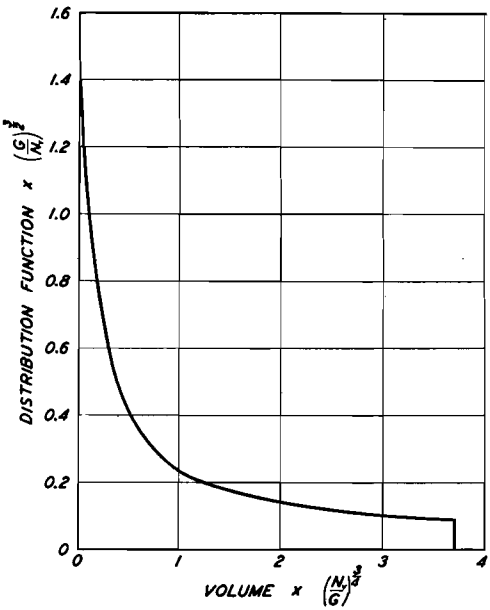

FIG. 7.—DISTRIBUTION CURVE IN SPACE FOR AVERAGE NODULE VOLUME.

The total number of nodules per unit volume of completely reacted sample, n_e, may be obtained by integrating equation 3 with respect to $\bar{\phi}$. The result is

$$n_e = 0.896(N_v/G)^{3/4} \qquad [4]$$

Since metallic samples are opaque, the distribution function in equation 3 is not directly applicable, but the distribution function for patches on a plane of polish can be derived from it on the assumption that the nodules are spheres whose volumes equal those of the corresponding nodules. With this assumption, the spacial distribution function, $\eta(\bar{\phi})$, which is in terms of volume, becomes $\psi(r)$ in terms of the corresponding

radius r; $\psi(r)$ is

$$\psi(r) = \frac{\sqrt{\pi/12}(N_v/G)^{3/2}e^{-2\alpha^4 r^2}}{\int_\alpha^\infty e^{-v^4}[(v-\alpha) - 2\alpha^3(v-\alpha)^2]dv} \quad [5]$$

where r is given by the relation $\bar{\phi} = \frac{4}{3}\pi r^3$ and the other terms have the same meaning as in equation 3. Equation 5 is plotted in Fig. 8; the method of plotting is described in detail in the discussion of Fig. 9. Although Figs. 7 and 8 both represent the distribution of nodules in space, they are of quite different shape because the distribution curve of Fig. 7 is plotted as a function of volume while that of Fig. 8 is plotted as a

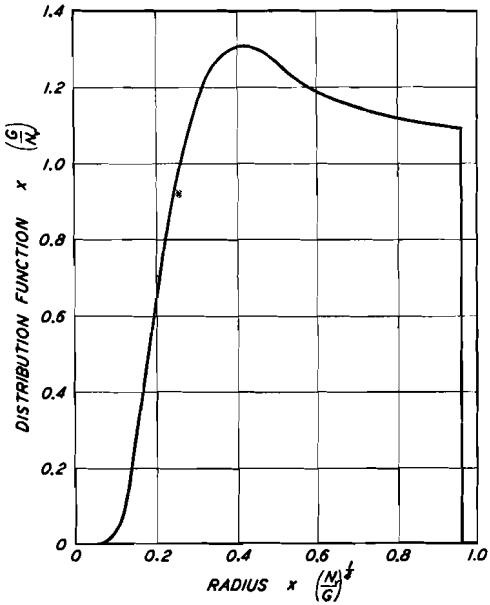

FIG. 8.—DISTRIBUTION CURVE IN SPACE FOR AVERAGE NODULE RADIUS.

function of radius. The distribution function, $\theta(\rho)$, for patches of radii ρ on a plane of polish is then given by[26]

$$\theta(\rho) = 2\rho \int_\rho^{r_{max.}} \frac{\psi(r)dr}{\sqrt{r^2 - \rho^2}} \quad [6]$$

where $\psi(r)$ is given by equation 5 and $r_{max.}$ is the radius of the largest sphere. Equation 6 is plotted in Fig. 9.

The number of patches of radius between ρ and $\rho + d\rho$ is the area under the curve between the abscissas ρ and $\rho + d\rho$, as illustrated in Fig. 9. This curve has been derived for the general case (all values of N_v and G), and thus the scales of the ordinate and abscissa axes are generalized. The abscissa is radius, and the units are as shown; to

illustrate, assuming $G = 16 \times 10^{-6}$ cm. per sec. and $N_v = 100$ per sec. per cm.^{3}, then $(G/N_v)^{1/4} = 0.02$ cm. The maximum radius is thus

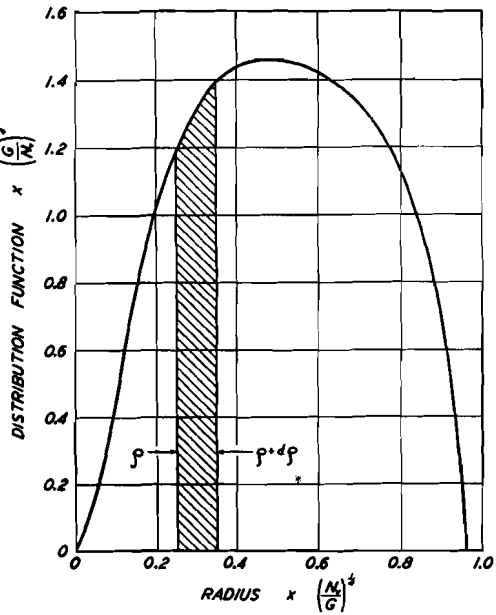

FIG. 9.—DISTRIBUTION CURVE ON PLANE OF POLISH FOR AVERAGE PATCH RADIUS.

$0.96 \times (G/N_v)^{1/4} = 0.96 \times 0.02$ cm. = 0.0192 cm.; intermediate radii are obtained in the same way; *i.e.*, by multiplying the abscissa values plotted in Fig. 9 by $(G/N_v)^{1/4}$. The ordinate values are obtained in a similar manner; thus, in the example given, the maximum value of the distribution function is $1.47 \times (N_v/G)^{3/4} = 1.47 \times 1/(0.02\,\text{cm.})^3 = 183{,}750$ per cm.^{3} Thus Fig. 9 is a master distribution curve for patches (nodule areas on a plane of polish) for a system that has reacted to completion by nucleation and growth with N_v and G constant throughout the reaction. Figs. 7 and 8 are also master plots from which distribution functions for particular values of N_v and G may be obtained by the simple calculations described for Fig. 9.

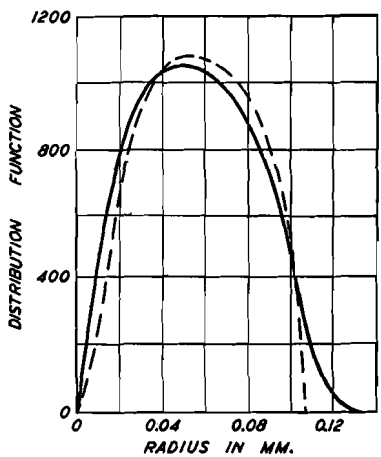

FIG. 10.—CORRESPONDENCE OF EXPERIMENTAL (FULL CURVE) AND CALCULATED DISTRIBUTION CURVE (DOTTED). Experimental and calculated curves obtained as described in Appendix C.

The total number of patches per unit area of a completely reacted sample, n_T, may be found by integrat-

ing equation 6 with respect to ρ. The result is

$$n_T = 1.01(N_v/G)^{\frac{1}{2}} \quad [7]$$

The distribution curve obtained by Scheil and Wurst[27] for the patch sizes in recrystallized Armco iron may be compared with the distribution curve calculated here. Changing the ordinate units so as to refer the data to a square millimeter area (Appendix C) and plotting the curve in the manner employed in Fig. 9, produces the curve shown in Fig. 10; the calculated distribution curve on this same figure is one derived for the same total number of patches. In general the agreement is good.

Application and Use of Analysis

The analysis given may be applied quantitatively to reactions for which the assumptions made in the derivation are valid. These are: (1) that the reaction proceeds by nucleation and growth, (2) that the distribution of nuclei is random, without regard for structure, and (3) that the rate of nucleation and the rate of growth remain constant throughout the reaction.

The application of the analysis to the process of freezing may be made only with certain limitations. When nucleation at the surface of the system is pronounced and extensive columnar growth occurs, the requirement of general nucleation is obviously not met. Similarly, in ordinary nonisothermal freezing, N_v and G will vary in a complicated fashion with the temperature, and this circumstance is difficult to provide for in an analytical way. It is possible also that the mobility of small nodules in a partially frozen melt should tend to decrease the importance of the impingement factor somewhat. But for the slow freezing of metal in the interior of an ingot, where equiaxed grains are obtained, the analysis may find an application.

The decomposition of austenite to pearlite in many cases shows pronounced grain-boundary nucleation,[2-8] and the nodules usually do not grow across the grain boundaries of the austenite matrix. This process, though meeting the other requirements, fails to meet those of general nucleation and of growth restricted only by impingement on other growing nodules. In some steels[25] general nucleation is pronounced, though apparently always accompanied by grain-boundary nucleation; in such cases the proper analysis must be a combination of that given above for general nucleation and that following in the next section on grain-boundary nucleation. It should also be pointed out that the formation of "lower" bainite from austenite almost beyond question is not a process of nucleation and growth,[25] and the analysis should not be applied to this.[22]

The application of the analysis to recrystallization is on more certain ground. This process is also one of nucleation and growth; in the recrys-

tallization of heavily deformed aggregates, nuclei appear to form at random and to grow without regard for the grain structure of the recrystallizing material. Nuclei form usually in twins or slip planes, but these regions are distributed sufficiently uniformly that the nucleation may be considered random. In some cases, however, N_v and G change during recrystallization; such a change in G has been shown for tin by Polanyi and Schmid[9] and for lead and zinc by Tammann and Crone,[10] though Karnop and Sachs[11] reported that G remains constant during the recrystallization of aluminum.

The reaction and distribution curves derived above may be used in the determination of N_v and G in any reaction that meets the requirements of the analysis. If the experimental reaction curve and the distribution curve of patch sizes are of the same shapes as the calculated reaction and distribution curves, it may be concluded that N_v and G remain constant throughout the course of the reaction; if the experimental reaction curve does not agree with the calculated curve, it may be concluded that either N_v or G or both are not constant; if N_v increases and G decreases during the reaction, the reaction curve may be indistinguishable from the reaction curve calculated for constant N_v and G, but the distribution curve would show a marked distortion, so that both should be used in applying this test.

If it is known that N_v and G remain constant for a given process, it is not necessary to have complete reaction and distribution curves for calculating N_v and G. If the fraction of transformation at a known time t is determined experimentally, the value of $\sqrt[4]{N_v G^3} \times t$ corresponding to this fraction of transformation is easily read from the reaction curve in Figs. 3 and 4; since the time is known, $\sqrt[4]{N_v G^3}$ is obtained. If the total number of patches per unit area on a polished surface is measured, the value of $(N_v/G)^{1/2}$ may be obtained from equation 7; from the values of $\sqrt[4]{N_v G^3}$ and $(N_v/G)^{1/2}$ determined in this way, the values of N_v and G may be calculated.

If it is known that N_v and G are constant, and if either one of these quantities is determined experimentally, the other may be calculated. This may be done either by counting the number of patches per unit area, which gives the value of $(N_v/G)^{1/2}$, or by determining the fraction of transformation in a given time, which gives the value of $\sqrt[4]{N_v G^3}$; by substituting in either of these quantities the one constant determined, the other may be calculated. This should greatly lighten the extreme labor required in the experimental determination of N_v and G.

Grain-boundary Nucleation

The Analysis

The derivation of the reaction equation when nucleation occurs exclusively at the grain boundary—as, for example, in the formation of pearlite

from austenite in certain steels,* presents special though not insurmountable difficulties. In this case we assume: (1) that the reaction proceeds by nucleation and growth, (2) that the rates of nucleation and growth remain constant throughout the reaction, (3) that nucleation is exclusively at grain boundaries, (4) that the matrix is composed of spherical grains of radius a, (5) that the nodules grow only into the grain in which the nuclei originated and do not cross grain boundaries, and (6) that the rate of transformation is retarded by impingement of growing nodules on one another and on grain boundaries. These are conditions for the formation of pearlite from austenite. Items 3, 4, 5 and 6 distinguish this case from the case of general nucleation.

We require an expression for the extent of reaction at any reaction time in terms of a rate of grain-boundary nucleation, N_s, expressed as number of nuclei per unit of time per unit of grain-boundary area; a rate of growth G; and a matrix grain size a, which provides for the impingement of growing nodules of reaction product and the resultant inactive impingement interface. The provision for impingement in this case is more difficult than in general nucleation, for there is no simple relation of impingement to the extent of reaction, and a different approach is required.

The derivation of the equation is given in Appendix D. The matrix is assumed to be constituted of spherical grains. The rate of transformation of a single grain is calculated and from this the rate of transformation of the aggregate of grains may be found. Nuclei are assumed to form at the surface of the grain and to grow inward; an arbitrary thin spherical shell within the grain and concentric with it is considered; the growing nodules intersect this shell; the rate of increase in the area of the shell contained within a particular nodule is calculated; multiplication of this rate by an impingement factor involving the area of the shell, the area of the shell contained within the particular nodule considered, and the fraction of the shell contained within all nodules, yields the rate of transformation of the shell due to the single nodule considered; integration of this rate for all times of nucleation yields the total rate of transformation of the shell. Integration of this gives the fraction of the shell transformed as a function of time (the fraction *untransformed* is given by equation 8*b*); integration of this over the whole grain gives the fraction of the grain transformed as a function of time (the fraction *untransformed* is given by equation 8*a*); correcting this equation for the most probable time of formation of the first nucleus in each grain yields the required equation for the fraction of transformation as a function of time, equation 8.

$$F(z) = 4\pi\lambda\int_0^z e^{-4\pi\lambda\alpha}\xi(z-\alpha)d\alpha \qquad [8]$$

* Bain[2-8] and Mehl.[25] A summary of the analysis to follow was given in the paper of reference 25.

where $$z = \frac{G}{a} \times t \qquad \text{and} \qquad \lambda = \frac{a^3 N_s}{G}$$

where $$\xi(z) = \begin{cases} 3\int_{1-z}^{1} y^2[1 - \omega(z,y)]dy & \text{when } z \leq 1 \\ 3\int_{0}^{1} y^2[1 - \omega(z,y)]dy & \text{when } z \geq 1 \end{cases} \qquad [8a]$$

where $$\omega(z,y) = \begin{cases} 1 & \text{when } 0 \leq z \leq (1-y) \\ \left[\frac{(1+y)^2 - z^2}{4y}\right]\left\{(y)^{(1+y-z)}\left[\frac{(1+y+z)}{(1+y-z)}\right]^{(1+y)}\left[\frac{(1+y)^2 - z^2}{4}\right]e^{2(1-y-z)}\right\}^{4\pi\lambda} & \text{when } (1-y) \leq z \leq (1+y) \\ 0 & \text{when } z \geq (1+y) \end{cases} \qquad [8b]$$

and where α and y are integration variables, whose limits are $0 \leq \alpha \leq \infty$ and $0 \leq y \leq 1$.

Equation 8 was evaluated numerically by Simpson's rule. The method is briefly as follows. The desired value of the parameter λ is chosen; for any assumed value of z, say z_1, a curve $\omega(z_1,y)$ can be calculated from equation 8*b*. Using this value of $\omega(z_1,y)$, which is a function of y, $\xi(z_1)$ can be calculated from equation 8*a*. Repeating this process for a series of values of z yields a curve $\xi(z)$ as a function of z. For any desired value of z, say z_2, a curve $\xi(z_2 - \alpha)$ can be constructed from $\xi(z)$; this curve can then be used to determine $F(z_2)$ from equation 8. Repeating this process for a series of values of z yields the desired reaction curve.

For values of λ not less than 3, the approximate formulas given previously[25] hold very well.

$$F(z) = \begin{cases} 3\int_{1-z}^{1} y^2[1 - g(y,z)]dy & \text{when } z \leq 1 \\ 3\int_{0}^{1} y^2[1 - g(y,z)]dy & \text{when } z \geq 1 \end{cases}$$

where $$g(y,z) = \begin{cases} \text{exp. } \{-\pi\lambda[z^3/3y - z/y \\ \quad (1-y)^2 + 2/3y(1-y)^3]\} & \text{when } (1-y) \leq z \leq (1+y) \\ 0 & \text{when } z \geq (1+y) \end{cases}$$

Equation 8 may be plotted in a number of ways. A family of curves could be plotted in which the grain size a and the rate of nucleation N_s were kept constant and various values assumed for the rate of growth G; another family could be plotted in which a and G were kept constant and N_s varied; and a third plotted in which G and N_s were kept constant and a varied; the use of these curves would then consist in finding which curve in these three families agreed with the experimental reaction curve. The multitude of comparison curves would render this method very

laborious. A much shorter method is to plot the equation in terms of the two factors in which it is written; namely, $\lambda = \frac{a^3 N_s}{G}$ and $z = G/a \times t$. Equation 8 is plotted in this fashion in Fig. 11, in which the time scale is linear, and in Fig. 12, in which the time scale is logarithmic, for a series of values of λ.

In applying this analysis, the plots given in Figs. 11 and 12 are sufficient for all purposes; it is not at all necessary to perform the computations outlined above, which have been described merely to demonstrate the method by which the plots were obtained. The use of these plots in the treatment of data is simple. They are master plots. The ordinate is $F(z)$, the fraction transformed. The abscissa is not simply time, but z, the actual time multiplied by G/a; the factor G/a is designated as the time-scale factor. The plot shows a family of curves, each characterized by a different value of $\lambda = \frac{a^3 N_s}{G}$. The value of this quantity determines the shape of the curve, and we shall designate this quantity λ as the shape factor. Curves for values of λ not shown may be obtained easily by interpolation. Any experimental reaction curve may be compared to these curves.

It is obvious from Figs. 11 and 12 that if N_s, G and a are known, the shape factor $\frac{a^3 N_s}{G}$ can be calculated and the shape of the curve determined; furthermore the time-scale factor G/a can be calculated and the horizontal or time extension of the curve determined. This should give a curve that coincides with the experimentally observed curve. Although a is readily determined, there have been no good determinations of N_s and G,[25] and an absolute comparison cannot be made on this basis. It has been shown, however, that curves of the form given in Figs. 11 and 12 can be fitted to experimental reaction curves with a high degree of perfection, as shown in Fig. 13.*

The number of nodules in each completely reacted grain of the matrix is a function only of the shape factor λ. This function is plotted in Fig. 14; the derivation of the equation is given in Appendix E. Since the volume of a single grain is $\frac{4}{3}\pi a^3$, the number of nodules per unit volume is found by multiplying the number of nodules read from Fig. 14 by $\frac{3}{4\pi a^3}$. This analysis cannot be extended, however, to the calculation

* The very slow initial rate of the decomposition of austenite has led some investigators to call this initial period an incubation or induction period, inferring that the system is "preparing" to react, that the major reaction has not yet begun. This is not necessary; it may be seen from Figs. 11 and 12 (and also from Figs. 1 and 2) that an initial slow rate is an inevitable result of the process of nucleation and growth. The logarithmic plotting exaggerates the initial slow rate.

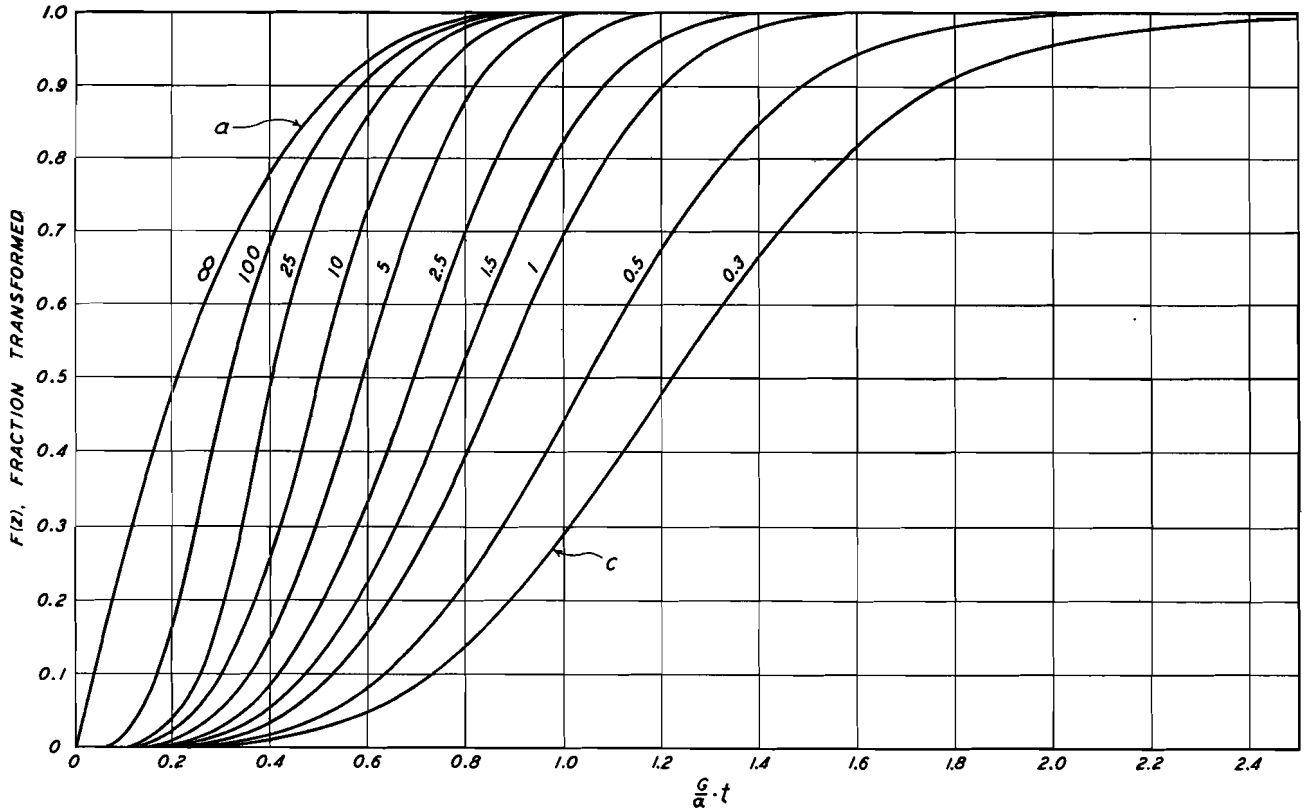

FIG. 11.—MASTER REACTION CURVES FOR GRAIN-BOUNDARY NUCLEATION, ABSCISSA SCALE LINEAR.

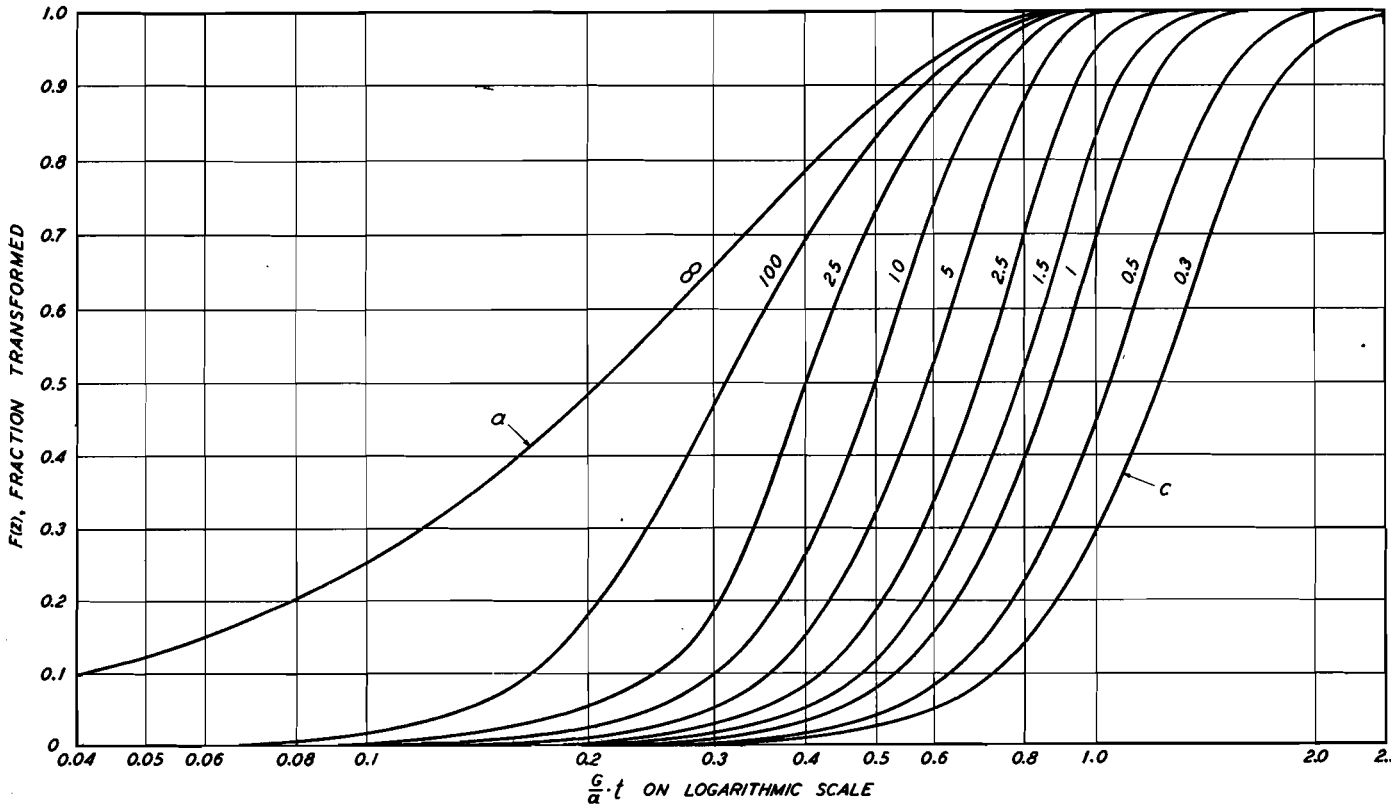

FIG. 12.—MASTER REACTION CURVES FOR GRAIN-BOUNDARY NUCLEATION, ABSCISSA SCALE LOGARITHMIC.

of the number of nodule intersections on the plane of polish—patches—nor to the distribution of patch areas, for the nodules in this case do not approximate spheres, as in general nucleation. Accordingly, no correlation between N_s, G, and a, and a distribution function of nodule size can be made until the statistical shape of the nodule is studied.

No one has made a careful study of the number of pearlite nodules that can form in a single grain of austenite, but it appears that the num-

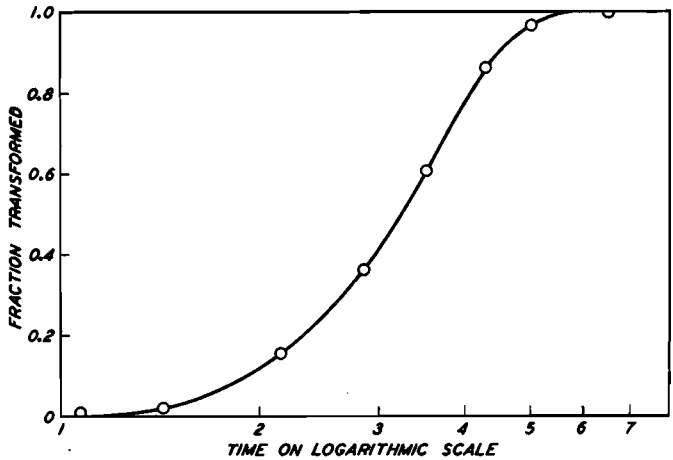

FIG. 13.—CORRESPONDENCE OF EXPERIMENTAL (FULL CURVE) AND CALCULATED REACTION CURVES (CIRCLES).

Experimental curve from Fig. 9, E. S. Davenport and E. C. Bain, *Transactions*, Amer. Soc. Metals (1934) **22**, 894. Calculated curve obtained as described in text. Abscissa scale logarithmic.

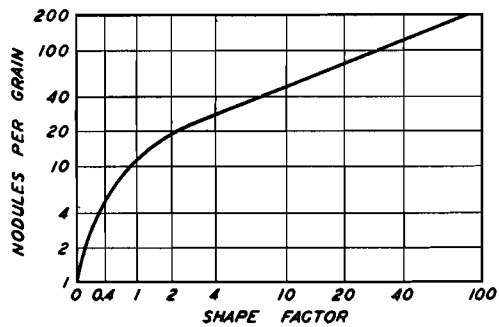

FIG. 14.—RELATION OF NUMBER $\bar{n}$ OF NODULES PER GRAIN TO SHAPE FACTOR λ.

The abscissa is log $(1 + \lambda)$. The ordinate corresponding to any value of $\bar{n}$ is proportional to log $\bar{n}$.

ber rarely, if ever, falls below 4 or 5, corresponding to a value of λ of approximately 0.3. Since the discussion of the effect of changes in N_s, G, and a on the shape of the reaction curve which follows is limited to the formation of pearlite from austenite, curves with shape factors under

0.3 will not be considered. For reactions other than the austenite-pearlite eutectoid decomposition, lower values of λ may have to be employed.

Effect of Grain Size

The effect of grain size may be sought by inquiring what the effect of increasing the grain size a will be upon the shape of the curve and upon the time scale. It can be seen from Fig. 11 that increasing a will increase the factor $\frac{a^3 N_s}{G}$ and will alter the shape of the curve toward that of curve (*a*); and conversely, a decrease in a will alter the shape of the curve toward that of curve (*c*); samples of the same steel with different grain sizes will therefore exhibit reaction curves of somewhat different shapes. With increasing grain size the distance the nodule must traverse to reach the center of the grain becomes greater, and this increases the reaction time. Thus an increase in a decreases the value of the time-scale factor G/a, and the time of reaction is increased. The grain size in commercial heat-treating steels varies essentially between American Society for Testing Materials numbers 10 and 1, corresponding to a range in a of 1 to 23. Increasing a by a factor of 23, and maintaining N_s and G constant, will increase the total reaction time by from 5 to 23 times, depending on the particular values of N_s and G obtaining.

The effect of grain shapes other than spheres is in general to increase the rate of reaction, since any other shape has a greater ratio of grain surface to grain volume and an increase in surface area engenders an increase in reaction rate. Mixed grain sizes, the so-called "duplex" grain structure, often occur. As shown in Fig. 11, the *shape* of the reaction curve varies with grain size, and the *displacement* of the curve on the time axis also varies. It would be expected that the reaction curve for a steel with mixed grain size would lie between those for the largest and smallest grain sizes in the sample, and this is true, but the curve is not identical with the curve calculated for the *average* grain size—it varies from this both in shape and (to a minor degree) in position with respect to the time axis, as shown in Fig. 15. A consideration of the phenomena at play in a duplex structure will suggest what this variation should be: the small grains will react quickly, and this will displace the first part of the curve upward (increasing percentage of reaction), whereas the large grains will react relatively slowly, and this will displace the latter part of the reaction curve downward (decreasing percentage of reaction). The actual effect of a duplex structure depends on the particular distribution of grain sizes present; it is not the same when only grain sizes No. 2 and No. 6 are present as when all grain sizes from No. 2 to No. 6 are present. In the first case the reaction curve will not be smooth—i.e., the small grains will have reacted almost completely before the large ones have reacted appreciably, and there may be a hump in the

reaction curve as a result. If the mixture of grain sizes is continuous, the reaction curve will be smooth. The disposition of the curves for different grain sizes shown in Fig. 15 depends on the relative values of N_s and G. Thus, the higher the value of the ratio N_s/G, the greater will be the separation of the curves for the different grain sizes.

Effect of Rate of Nucleation

Any discussion of the effects of rate of nucleation and rate of growth on the reaction curve is complicated by the fact that any influence that alters one often alters the other. Thus, while nonmetallic inclusions such as alumina probably affect only the rate of nucleation, alloying elements

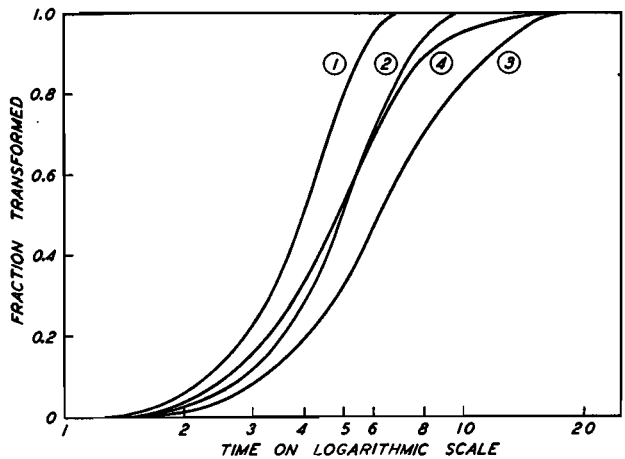

FIG. 15.—SHOWING EFFECT OF GRAIN SIZE AND EFFECT OF MIXED GRAIN SIZE ON REACTION CURVE.

Curve 1 is for A.S.T.M. grain size No. 6, curve 2 for grain size No. 4, curve 3 for grain size No. 2, curve 4 for a mixture of equal parts of grain sizes Nos. 6, 4 and 2. Note that reaction curve for mixture, curve 4, is not identical with reaction curve for average grain size, No. 4, curve 2.

probably exert an influence on both the rate of nucleation and the rate of growth. Variations in the rate of nucleation N_s will have no effect on the time-scale factor G/a, and will affect the reaction curve only by altering its shape. An increase in N_s will alter the shape of the curve toward that of curve (*a*), Fig. 11; the curve is thus displaced upward and correspondingly the time for a given percentage of reaction will be shorter by the amount of lateral displacement, right to left, which this incurs. It is a striking result of this analysis that altering the shape factor between 0.3 and ∞ results in a decrease in the time of reaction of only 70 per cent. If the grain size and the rate of growth are kept constant, and this variation in λ is effected by changing the rate of nucleation alone, the greatest possible variation in the rate of nucleation can have only a relatively small effect on the rate of reaction.

Effect of Rate of Growth

It can be seen from Fig. 11 that increasing G will alter the shape of the reaction curve toward that of curve (c), and decreasing G, toward that of curve (a); increasing G will also alter the time-scale factor, displacing the reaction curve toward shorter times. Any change in G produces opposite and nearly equal effects to those produced by the same change in a.

The chief factors in determining the rate of reaction are the grain size a and the rate of growth G; as stated, N_s is of much less influence relatively. Although the effects of variations in a and G are nearly equal though opposite, in reality G is a far more important variable, for it can be varied over a very much greater range. In commercial steels the grain size varies essentially between A.S.T.M. numbers 1 and 10, corresponding to a range in a of 1 to 23; but G can be varied over a very wide range, a range of many orders of magnitude, either by altering the temperature of reaction or, more important, by the addition of alloying elements. It is in this circumstance that lies the reason for the fact that the effect of grain size on the rate of reaction is a minor one compared to the effect of alloying elements.

The analysis of the reaction curve for the case where N_s is very low compared to G is interesting. In this case the generation of one nucleus in a grain results in the complete reaction of that grain before another grain is nucleated. The rate of reaction will thus be proportional to the rate of nucleation, which in turn is proportional to the number of grains still available for nucleation; that is, to the number of unreacted grains. This will accordingly furnish a reaction curve identical with that for a first-order reaction. But only in this very exceptional case will the first-order reaction curve be reproduced in form.

Conditions for Identical Reaction Curves

Two identical reaction curves (both with respect to shape and time) will be obtained when the two factors a^3N_s/G and G/a are identical in the two steels. The conditions under which this is possible can readily be appraised. For a given steel at a fixed reaction temperature, both N_s and G are constant, and only a can be varied; a cannot be varied to obtain identical constants and thus to obtain identical reaction curves. For a given steel reacting at a series of temperatures, N_s, G, and a are all variable, but in order to get identical factors and therefore identical reaction curves, N_s and G would have to change with temperature in opposite directions which, as has been shown,[25] is not observed in the formation of pearlite. For two different steels reacting at a series of temperatures, N_s, G, and a are again all variable, and it is possible that the stated condi-

tions can be met; coincidental reaction curves are theoretically possible and will be found if proper values of N_s, G and a appear.

The effect of variation in N_s and G during reaction can be discussed qualitatively; a quantitative discussion would require a knowledge of the type of such variation which is not available. When such data become available the appropriate modification of the analysis given in Appendix D can be made. A considerable increase in N_s will result in a relatively small effect on the reaction curve, since it has been shown that the maximum possible variation in time of reaction for maximum variation in N_s is only 70 per cent (note that this is for an increase in N_s for grain-boundary nucleation alone and does not pertain to any variation in intragranular nucleation). Variation in G, however, will exert an important influence on the rate of reaction since this will affect the time-scale factor.

Uses of Analysis

The analysis is of value in the experimental study of isothermal reaction rates, for it may be used greatly to facilitate the determination of the basic constants N_s and G, the rate of nucleation and the rate of growth.

1. With a known, approximate values of N_s and G can be obtained from the isothermal reaction curve alone if the reaction curve is determined accurately. The procedure is as follows: Plot the experimental curve with time logarithmic to the same scale as given in Fig. 12 (the same abscissa distance for each power of 10); superimpose the experimental and the master curves in Fig. 12, and shift curves laterally until the experimental curve is brought into coincidence with one of the master curves; this will give the value of a^3N_s/G. Choose any point on the time axis; read the value of $G/a \times t$ at this point from the master curve and the value of t from the experimental curve; with a known, G can be calculated; since a^3N_s/G has been determined, and since a and G are known, N_s can be calculated. The errors will accumulate in N_s, but since N_s is less important than either G or a this is not disturbing.

2. If more accurate values of N_s than those given in paragraph 1 are desired, an experimental determination of G is required. The procedure is as follows: With G and a known, the experimental curve may be plotted on Fig. 12 directly by multiplying the experimental times by G/a, and the curve with which it coincides selected; from the value of a^3N_s/G for this curve and the known values of a and G, N_s may be calculated.

3. If more accurate values of G than those given in paragraph 1 are desired, an experimental determination of N_s is required. The procedure is as follows: The experimental curve may be fitted to the master curve as in (1); equally good fits can be obtained with λ values varying within a narrow range. For each λ value within this range a value of N_s and G may be calculated as in (1); from this series the N_s value closest to the

experimentally determined N_s value may be selected, and the accompanying G value is that desired.

In determining rates of nucleation and rates of growth, therefore, the analysis should be of assistance in shortening experimental studies. The analysis applies only, it must be emphasized, to a process that proceeds by nucleation at grain boundaries exclusively and by radial growth from these nuclei. In applying it, it is necessary first to ascertain that the process conforms to these conditions. The formation of bainite at low temperatures and the formation of martensite in steels, though perhaps starting at grain boundaries, do not proceed by radial growth, and accordingly the analysis must not be applied to these reactions. The fact that the formation of bainite at low temperatures gives a reaction curve very similar in appearance to that for the formation of pearlite is thus wholly deceptive. For reactions in steel the analysis applies therefore only to the formation of pearlite.

No studies of the statistical shape of pearlite nodules have been made, and the patch-area distribution curve accordingly has not been calculated, but it seems possible to make a successful study of this sort and to derive the desired distribution curve. If a method were available for determining the number of patches after complete reaction, a relation between this number and N_s, G, and a could be derived, and this would be of assistance in determining N_s and G in a manner comparable to the method used in the first section.

The possible shapes of reaction curves for grain-boundary nucleation as given in Fig. 11 include a curve for $\lambda = \infty$ which starts with maximum velocity, whereas the reaction curve for general nucleation always starts with a zero velocity and then accelerates. An experimental curve of the shape given by the curve $\lambda = \infty$ in Fig. 11 may thus be taken as proof of grain-boundary nucleation, whereas curves of any other shape will not in themselves distinguish between the two types of nucleation. The reaction curve for the decomposition of the phase "FeO"[15] is of the shape $\lambda = \infty$ in Fig. 11, and it may be concluded that nucleation in this transformation is restricted to the grain boundary.

Summary

An analytical expression is derived for the rate of reaction in a reaction proceeding by nucleation and growth when nucleation occurs without regard for matrix structure and the nuclei tend to grow into spherical nodules. The effects upon the reaction curve of variations in the rate of nucleation N_v, and in the rate of growth G, have been derived from the analytical expression. Distribution curves are derived for the sizes of nodules and for the corresponding areas on the surface of polish. The application of the analysis to the process of freezing and recrystallization is discussed. The calculation of N_v and G from easily obtained experi-

mental data is described. If N_v or G is known, the other may be calculated from fewer experimental data.

An analytical expression is derived for the rate of reaction in a reaction proceeding by nucleation and growth when nucleation is restricted to the grain boundaries and the nuclei tend to grow to half-spherical nodules. The effects upon the reaction curve of variations in matrix grain size a, in the rate of grain-boundary nucleation N_s, and in the rate of growth G, have been derived from the analytical expression. Conditions for identical reaction curves are given. The application of the analysis to actual reactions, particularly the formation of pearlite from austenite, is discussed. It is shown: (1) that if a is known and the experimental reaction curve known accurately, N_s and G can be calculated with fair accuracy, and (2) that if a and the experimental reaction curve are known and either N_s or G is known, the other can be calculated with improved accuracy.

These analyses serve not only to reproduce the form of isothermal reaction curves in terms of the constants $N(N_v$ or $N_s)$ and G, but serve also to assist in the determination of these basically important constants.

Acknowledgment

The authors wish to acknowledge the granting of a graduate fellowship to one of them by the Molybdenum Corporation of America. This generosity has made the present work possible.

References

1. G. Tammann: States of Aggregation. Translation by R. F. Mehl. New York, 1925. D. Van Nostrand Co.
2. E. S. Davenport and E. C. Bain: *Trans.* A.I.M.E. (1930) **90,** 117.
3. E. C. Bain: *Trans.* A.I.M.E. (1932) **100,** 13.
4. E. C. Bain: *Trans.* Amer. Soc. Metals (1932) **20,** 385.
5. E. C. Bain: *Year Book* Amer. Iron and Steel Inst. (1934) 86–119.
6. J. R. Vilella, G. E. Guellich and E. C. Bain: *Trans.* Amer. Soc. Metals (1936) **24,** 225.
7. J. G. Zimmerman, R. H. Aborn and E. C. Bain: *Trans.* Amer. Soc. Metals (1937) **15,** 755.
8. E. C. Bain: *Jnl.* Iron and Steel Inst. (1938) **138,** 33P.
9. M. Polanyi and E. Schmid: *Ztsch. Physik* (1925) **32,** 684.
10. G. Tammann and W. Crone: *Ztsch. anorg. allg. Chem.* (1930) **187,** 289.
11. R. Karnop and G. Sachs: *Ztsch. Physik* (1930) **60,** 464.
12. Series by F. Wever and collaborators, beginning 1930: F. Wever and N. Engel, *Mitt.* K.W.I. Eisenforschung, Düsseldorf (1930) *Abh.* 150. The first paper on isothermal reaction rates was by F. Wever and H. Lange: *Ibid.* (1932) *Abh.* 201. The most recent paper was by F. Wever and A. Rose: *Ibid.* (1938) *Abh.* 359.
13. C. S. Smith and W. E. Lindlief: *Trans.* A.I.M.E. (1933) **104,** 69.
14. W. Fraenkel and W. Goez: *Ztsch. Metallkunde* (1925) **17,** 12.
15. G. Chaudron and H. Forester: *Compt. rend.* (1924) **178,** 2173–2176.

16. D. L. McBride, C. H. Herty, Jr. and R. F. Mehl: *Trans.* Amer. Soc. Metals (1936) **14,** 281.
17. E. Cohen and C. van Eijk: *Ztsch. phys. Chem.* (1899) **30,** 616.
18. W. Fraenkel and W. Goez: *Ztsch. anorg. Chem.* (1925) **144,** 45.
19. H. Krainer: (*a*) *Archiv Eisenhüttenwesen* (1936) **9,** 619; (*b*) *Ztsch. Elektrochem* (1937) **43,** 503–509.
20. J. B. Austin and R. L. Rickett: A.I.M.E. *Tech. Pub.* 964 (*Metals Tech.* Sept. 1938).
21. F. Wever and H. Hänsel: *Mitt.* K. W. I. Eisenforschung, Düsseldorf (1937) *Abh.* 318.
22. G. Tammann: *Ztsch. anorg. allg. Chem.* (1933) **214,** 407.
23. G. B. Upton: *Trans.* Amer. Soc. Metals (1934) **22,** 690.
24. F. v. Göler and G. Sachs: *Ztsch. Physik* (1932) **77,** 281–286.
25. R. F. Mehl: The Physics of Hardenability. Amer. Soc. Metals Preprint (Oct. 1938).
26. A. Huber: *Ztsch. Physik* (1934–1935) **93,** 227.
27. E. Scheil and H. Wurst: *Ztsch. Metallkunde* (1936) **28,** 340–343.